Residual-Mean Solutions for the Antarctic Circumpolar Current and Its Associated Overturning Circulation

JOHN MARSHALL AND TIMOUR RADKO

Massachusetts Institute of Technology, Cambridge, Massachusetts

(Manuscript received 21 May 2002, in final form 25 March 2003)

ABSTRACT

Residual-mean theory is applied to the streamwise-averaged Antarctic Circumpolar Current to arrive at a concise description of the processes that set up its stratification and meridional overturning circulation on an f plane. Simple solutions are found in which transfer by geostrophic eddies colludes with applied winds and buoyancy fluxes to determine the depth and stratification of the thermocline and the pattern of associated (residual) meridional overturning circulation.

1. Introduction

Thermocline theory offers plausible explanations of the structure of midlatitude ocean gyres in linear vorticity and Sverdrup balance as reviewed, for example, in Rhines (1993) and Pedlosky (1996). Theories of ocean currents in zonally unblocked geometries such as the Antarctic Circumpolar Current (ACC) are much less well developed, however. In the absence of meridional boundaries, Sverdrup balance no longer applies and it is much less obvious how a meridional circulation is maintained. Furthermore, just as in zonal-average theory of the atmosphere, geostrophic eddy transfer in the ACC plays a central role in its integral balances of heat, momentum, and vorticity—see, for example, McWilliams et al. (1978), Bryden (1979), Marshall (1981), de Szoeke and Levine (1981), Johnson and Bryden (1989), Gille (1997), Marshall (1997), Phillips and Rintoul (2000), Karsten et al. (2002), Bryden and Cunningham (2003). For a recent review of observations and theories of the ACC, see Rintoul et al. (2001).

In this paper, we put forward a simple theory of the ACC and its associated meridional overturning circulation that makes use of zonal average residual-mean theory. Key observations of the Southern Ocean are summarized in Fig. 1 in which we show the time-mean surface elevation, a schematic of the meridional overturning circulation (MOC), the streamwise-averaged buoyancy distribution, and the thermal wind. We suppose, as sketched in Fig. 2, that westerly winds τ drive the ACC eastward and, through associated Ekman currents, induce an Eulerian meridional circulation $\overline{\Psi}$ (the Deacon cell, see Doos and Webb 1994) that acts to overturn isopycnals, enhancing the strong frontal region maintained by air–sea buoyancy forcing B. The potential energy stored in the front is released, we imagine, through baroclinic instability, and the ensuing eddies induce an overturning circulation Ψ^* that tends to restore the isopycnals to the horizontal (see Fig. 2). In the theory presented here, it is the interplay of the advection of buoyancy in the meridional plane by $\overline{\Psi}$ and Ψ^* that sets the structure of the ACC.

We suppose the following.

1) Transfer by geostrophic eddies, balancing momentum and buoyancy input at the surface, sets the stratification and vertical extent of the ACC. This assumption yields predictions for the depth of penetration and stratification of the ACC and its baroclinic transport as a function of wind and buoyancy forcing and eddy transfer.
2) There is an approximate balance between $\overline{\Psi}$ and Ψ^*; the MOC of the ACC is the ''residual'' circulation $\Psi_{\text{res}} = \overline{\Psi} + \Psi^*$ that advects buoyancy (and other tracers) in the meridional plane to offset sources and sinks. Here we will solve for the pattern of Ψ_{res} given the pattern of wind and buoyancy forcing at the surface and assuming a closure for Ψ^*.

Before going on, we emphasize that here we develop an ''f plane'' theory of the ACC—there is no account taken of the β effect. The relation of this study to previous β-plane investigations is discussed as we proceed and in the conclusions.

Our paper is set out as follows. In section 2 we formulate the problem by developing and applying resid-

Corresponding author address: John Marshall, Department of Earth, Atmosphere and Planetary Sciences, Massachusetts Institute of Technology, Rm. 54-1526, 77 Massachusetts Ave., Cambridge, MA 02139.
E-mail: marshall@gulf.mit.edu

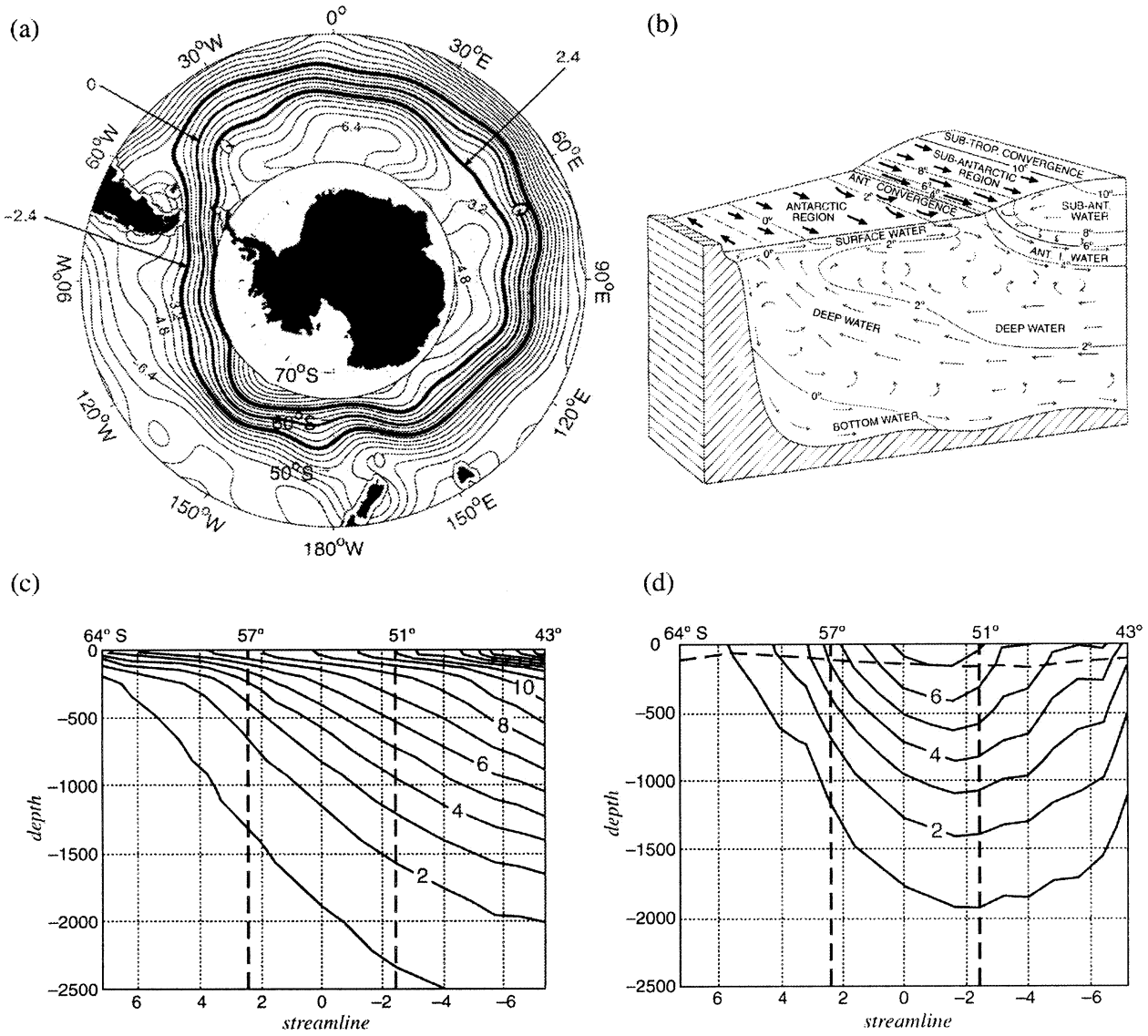

FIG. 1. Key observations of the ACC: (a) the time-mean surface elevation measured from altimetry. Contour interval is 0.8×10^4 m^2 s^{-1}. The bold lines mark the boundaries of circumpolar flow. (b) A schematic of the currents and overturning circulation in the Antarctic region modified from Fig. 164 of Sverdrup et al. (1942). (c) The streamwise-average buoyancy distribution computed from gridded hydrography; contour interval is 10^{-3} m s^{-2}. The vertical dotted lines denote the average latitude of circumpolar flow marked in (a). (d) The thermal wind velocity computed from gridded hydrography by integration of the thermal wind assuming zero current at the bottom; contour interval is 10^{-2} m s^{-1}. Modified from Karsten and Marshall (2002b).

ual-mean theory to the ACC. In section 3 we find solutions for the vertical structure of the ACC and its associated MOC. In section 4 we discuss and conclude.

2. Residual-mean theory applied to the ACC

We assume at the outset that ''zonal average'' theory has relevance to the ACC. However, rather than averaging along latitude circles, we reference our along-stream coordinate to a mean surface geostrophic contour (see Fig. 1a). Thus our zonal average, $\overline{()}^x$, ''follows the stream,'' as in de Szoeke and Levine (1981), rather than a latitude circle. Eddy fluxes normal to these contours are then by construction due to transient rather than standing eddies—see Marshall et al. (1993).

a. Residual-mean balances of momentum and buoyancy

1) BUOYANCY

The time-mean steady buoyancy equation can be written in the familiar form:

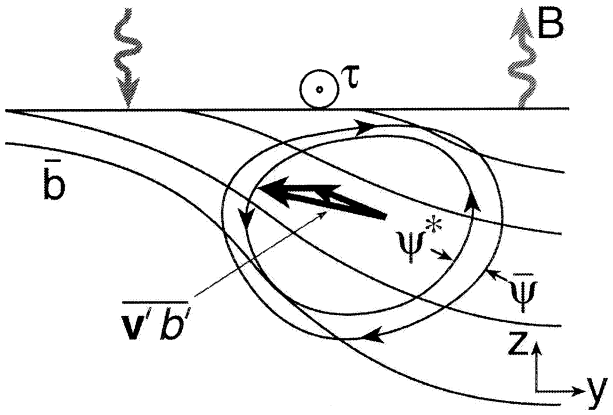

FIG. 2. Schematic diagram of the Eulerian mean ($\overline{\Psi}$) and eddy-induced transport (Ψ^*) components of the Southern Ocean meridional overturning circulation driven by wind (τ) and buoyancy (B) fluxes. The associated velocity is computed from the streamfunction as $(u, v) = (-\partial\Psi/\partial z, \partial\Psi/\partial y)$, where y is a coordinate pointing northward and z points upward. The sloping lines mark mean buoyancy surfaces $\overline{b}$. The eddy buoyancy flux $\overline{v'b'}$ is resolved into a component in the $\overline{b}$ surface and a horizontal (diapycnal) component.

$$\overline{v}\frac{\partial\overline{b}}{\partial y} + \overline{w}\frac{\partial\overline{b}}{\partial z} + \frac{\partial}{\partial y}(\overline{v'b'}) + \frac{\partial}{\partial z}(\overline{w'b'}) = \frac{\partial B}{\partial z}, \quad (1)$$

where $(\overline{v}, \overline{w})$ is the Eulerian mean velocity in the meridional plane, $\overline{b}$ is the mean buoyancy, and variables have been separated into mean (zonal and time) quantities and perturbations from this mean caused by transient eddies. Here, for simplicity, we have adopted a Cartesian coordinate system (see Fig. 2). Note that we are in the Southern Hemisphere: x increases eastward, y increases equatorward, z increases upward, and the Coriolis parameter $f < 0$. In Eq. (1) the buoyancy forcing from air–sea interaction and small-scale mixing processes has been written as the divergence of a buoyancy flux B.

Our goal now is to express Eq. (1) in terms of the residual circulation Ψ_{res}:

$$\Psi_{res} = \overline{\Psi} + \Psi^*, \quad (2)$$

where $\overline{\Psi}$ is the overturning streamfunction for the Eulerian mean flow and Ψ^* is the streamfunction for the overturning circulation associated with eddies (see Fig. 2 and caption). The key step is to note that if the eddy flux $\overline{\mathbf{v}'b'}$ lies in the $\overline{b}$ surface, then $\nabla\cdot\overline{\mathbf{v}'b'}$ can be written entirely as an advective transport, $\mathbf{v}^*\cdot\nabla\overline{b}$, where, following Held and Schneider (1999), $\mathbf{v}^*$ is defined in terms of a streamfunction Ψ^* given by

$$\Psi^* = -\frac{\overline{w'b'}}{\overline{b}_y}. \quad (3)$$

Here $\overline{w'b'}$ is the vertical eddy buoyancy flux and $\overline{b}_y$ is the mean meridional buoyancy gradient.

In more precise terms, to express Eq. (1) in terms of Ψ_{res}, we eliminate $(\overline{v}, \overline{w})$ using Eqs. (2) and (3) to obtain[1]

$$J_{y,z}(\Psi_{res}, \overline{b}) = \frac{\partial B}{\partial z} - \frac{\partial}{\partial y}[(1-\mu)\overline{v'b'}], \quad (4)$$

where $J_{y,z}(\Psi_{res}, \overline{b}) = (\Psi_{res})_y\overline{b}_z - (\Psi_{res})_z\overline{b}_y = \mathbf{v}^*\cdot\nabla\overline{b}$ and μ is given by

$$\mu = \left(\frac{\overline{w'b'}}{\overline{v'b'}}\right)\left(\frac{1}{s_\rho}\right). \quad (5)$$

Here

$$s_\rho = -\overline{b}_y/\overline{b}_z \quad (6)$$

is the slope of mean buoyancy surfaces. The parameter μ controls the magnitude of the diapycnal eddy flux: if $\mu = 1$, then the eddy flux is solely along $\overline{b}$ surfaces, the diapycnal horizontal component vanishes, and the advective transport captures the entire eddy flux; if $\mu = 0$, horizontal diapycnal eddy transport makes a contribution to the buoyancy budget. Diagnosis of the eddy-resolving ''polar cap'' calculations presented in Karsten et al. (2002) shows that the interior eddy flux is indeed closely adiabatic but that, as the surface is approached, $\overline{w'b'}$ tends to zero, leaving a horizontal eddy flux directed across $\overline{b}$ surfaces. The implications of these diabatic eddy fluxes are studied in section 3f. Elsewhere in our study we assume that all diabatic eddy fluxes are zero.

Note the following.

1) Streamfunction Ψ^*, Eq. (3), is defined so that, in the limit of adiabatic eddies, vanishing small-scale mixing, and air–sea buoyancy fluxes ($\mu = B = 0$), Eq. (4) reduces to $J(\Psi_{res}, \overline{b}) = 0$. Then $\overline{b}$ is advected by Ψ_{res}, suggesting that classic inferences of overturning in the Southern Ocean based on tracer distributions (see Fig. 1b) are sketches of the residual, rather than of the Eulerian mean flow.
2) Streamfunctions Ψ^*, $\overline{\Psi}$, and hence Ψ_{res} unequivocally vanish at the surface because $\overline{w} = w' = 0$ there.

2) MOMENTUM

We now wish to express the momentum balance in terms of residual, rather than Eulerian-mean velocities. This is desirable because the buoyancy equation [Eq.

[1] To arrive at Eq. (4) from Eq. (1), decompose the eddy fluxes $(\overline{v'b'}, \overline{w'b'})$ into an along-$\overline{b}$ component $(\overline{w'b'}/s_\rho, \overline{w'b'})$ and the remaining horizontal component $(\overline{v'b'} - \overline{w'b'}/s_\rho, 0)$ (see Fig. 2). The divergence of the along-$\overline{b}$ component is then written as an advective transport

$$\nabla\cdot(\overline{w'b'}/s_\rho, \overline{w'b'}) = \overline{v}^*\overline{b}_y + \overline{w}^*\overline{b}_z = J(\Psi^*, b),$$

where Ψ^* is given by Eq. (3). This is combined with mean flow advection in Eq. (1) to yield the lhs of Eq. (4). The divergence of the diapycnal (horizontal) eddy flux leads to the last term on the rhs of Eq. (4).

(4)], to which the momentum equation is intimately linked, is most succinctly expressed in terms of residual velocities; the momentum and buoyancy equations must be discussed together.

The statement of Eulerian-mean zonal-average zonal momentum balance is, in the steady state (remembering that $\overline{p_x} = 0$, etc.),

$$-f\overline{v} = \overline{F}, \tag{7}$$

where f is the Coriolis parameter, $\overline{v}$ is the Eulerian-mean meridional velocity, and $\overline{F}$ combines together momentum sources and sinks and momentum fluxes $\overline{uv}$, such as $-\nabla\cdot(\overline{vu})$ terms. To express Eq. (7) in terms of the residual meridional velocity

$$v_{\text{res}} = \overline{v} + v^*,$$

where

$$\overline{v} = -\frac{\partial\overline{\Psi}}{\partial z} \quad \text{and} \quad v^* = -\frac{\partial\Psi^*}{\partial z}, \tag{8}$$

we add $-fv^*$ to both sides of Eq. (7). The resulting residual momentum balance can be written as

$$f\frac{\partial\Psi_{\text{res}}}{\partial z} = \overline{F} + f\frac{\partial\Psi^*}{\partial z}, \tag{9}$$

where we have used Eq. (2) and Ψ^* is chosen as in Eq. (3) to ensure that the residual buoyancy balance, Eq. (4), takes on a simple form.

To make further progress, we now make some simplifying assumptions.

b. Simplified system

In the interior of the ACC we suppose that 1) buoyancy forcing (due both to convection and mixing processes) vanishes, that is, $B = 0$ in Eq. (4), and that 2) the eddy flux is directed entirely along $\overline{b}$ surfaces, that is, $\mu = 1$ in Eq. (4). Thus

$$J(\Psi_{\text{res}}, \overline{b}) = 0 \tag{10}$$

in the interior, implying that there is a functional relationship between Ψ_{res} and $\overline{b}$: $\Psi_{\text{res}} = \Psi_{\text{res}}(\overline{b})$. This functional relationship will be set, we suppose, in the surface mixed layer.

We suppose the following about the mixed layer: 1) It is vertically homogeneous and of constant depth h_m, as sketched in Fig. 3. Furthermore, we set entrainment fluxes at the base of the mixed layer to zero ($B_{-h_m} = 0$) and neglect the seasonal cycle. 2) Eddy fluxes have a diabatic component; μ in Eq. (4) varies from 0 at the surface to 1 at the base of the mixed layer—see Treguier et al. (1997) and Fig. 3.[2]

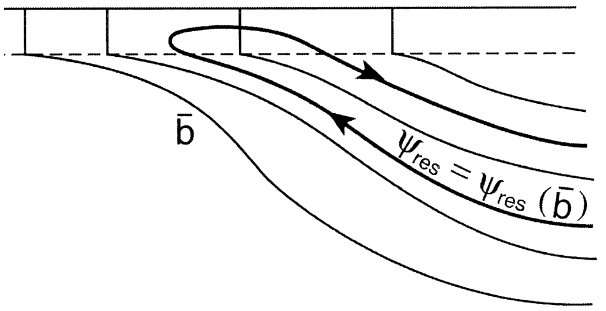

FIG. 3. The residual flow $\Psi_{\text{res}} = \overline{\Psi} + \Psi^*$ is assumed to be directed along mean buoyancy surfaces $\overline{b}$ in the interior but to have a diapycnal component in the mixed layer of depth h_m (denoted by the horizontal dotted line).

With these assumptions, the steady-state mixed layer buoyancy budget can be written as

$$-\frac{\partial\Psi_{\text{res}}}{\partial z}\frac{\partial b_o}{\partial y} = \frac{\partial B}{\partial z} - (1-\mu)\frac{\partial}{\partial y}\overline{v'b'},$$

where $b_o(y)$ is the mixed layer buoyancy. Integration over the depth of the mixed layer h_m, noting that $\Psi_{\text{res}} = 0$ at the surface, gives

$$\Psi_{\text{res}|z=-h_m}\frac{\partial b_o}{\partial y} = \tilde{B}_o, \tag{11}$$

where

$$\tilde{B}_o = B_o - (1-\mu)\int_{-h_m}^{0}\frac{\partial}{\partial y}\overline{v'b'}\,dz \tag{12}$$

is the net buoyancy supplied to the mixed layer by air–sea buoyancy fluxes and by lateral diabatic eddy fluxes. The relative importance of B_o and $\partial\overline{v'b'}/\partial y$ in the local buoyancy budget of the diabatic surface layer is not yet clear. Speer et al. (2000) argue (and show supporting observational evidence) that air–sea fluxes can provide the necessary warming to allow a surface flow directed away from Antarctica as suggested in Fig. 1b: indeed they diagnose the sense of Ψ_{res} from Eq. (11) using observations of $\tilde{B}_o$ (assuming that $\tilde{B}_o$ is dominated by surface heat fluxes). In theoretical calculations, Marshall (1997) also assumes that the eddy contribution in Eq. (12) is negligible. Calculations presented in section 3f below, however, suggest that diapycnal eddy fluxes could play an important role in the buoyancy budget of the surface layer in the ACC.

Equation (11) sets the functional relationship between Ψ_{res} and b_o. If $\tilde{B} > 0$ (corresponding to local buoyancy gain by the mixed layer), then, because $\partial b_o/\partial y > 0$, $\Psi_{\text{res}\,|\,z=-h_m} > 0$ and so (noting that $\Psi_{\text{res}\,|\,\text{surface}} = 0$) the flow in the mixed layer is directed equatorward. If the mixed-layer buoyancy gradient is constant, then, according to Eq. (11), the strength and sense of the residual circulation will be directly proportional to $\tilde{B}$ at each latitude.

In the momentum equation [Eq. (9)], we suppose that

[2] Note that it is likely that the depth h_m of the ''diabatic'' layer is not, in general, the mixed layer depth (A.-M. Tregueir 2001, personal communication). It is more likely that h_m at a given location is the depth of the deepest isopycnal that occasionally grazes the surface because of eddy dynamics or the seasonal cycle.

$\partial(\overline{uv})/\partial y$ terms can be neglected,[3] allowing $\overline{F}$ to be set equal to the vertical divergence of a stress, $\overline{F} = \partial\overline{\tau}/\partial z$. Then Eq. (9) can be written as

$$f\frac{\partial\Psi_{\text{res}}}{\partial z} = \frac{\partial\overline{\tau}}{\partial z} + f\frac{\partial\Psi^*}{\partial z}.$$

Integrating from the surface where $\Psi^* = \Psi_{\text{res}} = 0$ and $\overline{\tau} = \tau_o$ (the surface wind stress) through the surface Ekman layer to depth z in the interior, where $\overline{\tau} = 0$, we obtain

$$\Psi_{\text{res}}(z) = -\tau_o/f + \Psi^*(z). \tag{13}$$

Equation (13) is one of our key relations and equates the residual flow to the sum of an Eulerian circulation, the directly Ekman-driven current $-\tau_o/f$, and a flow associated with eddies, Eq. (3). The physical content of Eq. (13) is a statement of steady-state integral momentum balance: multiplying through by f, we see that the net Coriolis torque on the residual flow over the water column is balanced by wind stress applied at the surface and eddy form drag at the bottom. Note that in the ACC, $f < 0$ and $\tau > 0$, and so Ekman flow is directed equatorward at the surface: $\overline{\Psi} > 0$, as sketched in Fig. (2).

To proceed further, we must express Ψ^* in terms of $\overline{b}$. In other words, we must ''close'' for the eddy flux.

c. Closure for Ψ^*

If the eddies are ''adiabatic'' in the interior, then $\mu = 1$ in Eq. (5), and Eq. (3) can be written in terms of horizontal buoyancy fluxes as follows:

$$\Psi^* = -\frac{\overline{w'b'}}{\overline{b}_y} = \frac{\overline{v'b'}}{\overline{b}_z}, \tag{14}$$

yielding the more ''conventional'' definition of Ψ^*—see, for example, Andrews et al. (1987) and Gent and McWilliams (1990). We adopt the following simple closure for the interior eddy buoyancy flux:

$$\overline{v'b'} = -K\overline{b}_y,$$

where K is an eddy transfer coefficient that is assumed to be positive. Then Ψ^* can be written as

$$\Psi^* = \frac{\overline{v'b'}}{\overline{b}_z} = -K\frac{\overline{b}_y}{\overline{b}_z} = Ks_\rho, \tag{15}$$

where S_ρ is given by Eq. (6). Furthermore, if we suppose that K is itself proportional to the isopycnal slope [this assumption and its relation to the prescription of the horizontal variation of the Ks, suggested by Visbeck et al. (1997), is discussed in the appendix]:

$$K = k|s_\rho|, \tag{16}$$

where k is a positive scaling constant, then Ψ^* can be written as

$$\Psi^* = k|s_\rho|s_\rho. \tag{17}$$

In the ACC, Ψ^* is negative, that is, in the sense to return the isopycnals to the horizontal, balancing $\overline{\Psi}$ as sketched in Fig. (2).

3. Solutions for the ACC and its overturning circulation

Let us now draw together our key relations—Eqs. (11), (13), and (17)—and seek solutions. They are

$$\frac{\tau_o}{f} + \Psi_{\text{res}} = \Psi^* \quad \text{and} \quad \Psi^* = k|s_\rho|s_\rho, \tag{18}$$

where

$$\Psi_{\text{res}} = \Psi_{\text{res}}(b) \tag{19}$$

set in the mixed layer by Eq. (11) and s_ρ is given by Eq. (6).

Rearranging the above, we can write (for $s_\rho < 0$, the case considered here)

$$s_\rho = -\left[-\frac{\tau_o}{fk} - \frac{\Psi_{\text{res}}(b)}{k}\right]^{1/2}. \tag{20}$$

In that which follows, the system of Eqs. (18)–(20) will be solved for a given surface pattern of $\tau_o(y)$, $\tilde{B}_o(y)$, and $b_o(y)$.

a. Solution technique

Any physically meaningful model of the ACC should be characterized by the poleward shallowing of the thermocline in which $s_\rho < 0$ (see Fig. 1c), and therefore we consider only the solution branch corresponding to the negative sign in Eq. (20). The equation for the slope [Eq. (20)] is rewritten as a first-order partial differential equation in $\overline{b}$ using Eq. (6):

$$\overline{b}_y - \left[-\frac{\tau_o(y)}{fk} - \frac{\Psi_{\text{res}}(\overline{b})}{k}\right]^{1/2}\overline{b}_z = 0. \tag{21}$$

Despite the seemingly complicated form of its coefficients, this equation can be easily integrated along characteristics, since $\tau_o(y)$ is prescribed and $\Psi_{\text{res}}(\overline{b})$ can be evaluated at the base of the mixed layer using Eq. (11).

The characteristic velocities v_c and w_c are

$$\frac{dy}{dl} = v_c = 1$$

$$\frac{dz}{dl} = w_c = -\left[-\frac{\tau_o(y)}{fk} - \frac{\Psi_{\text{res}}(b)}{k}\right]^{1/2}, \tag{22}$$

and, of course, Ψ_{res} and $\overline{b}$ do not change at a point moving along the characteristic

$$d\Psi_{\text{res}}/dl = 0 \quad \text{and} \quad d\overline{b}/dl = 0,$$

where l is the distance along a characteristic.

[3] This is a very good approximation in the ACC—see the estimates of $\overline{u'v'}$ based on float data by Gille (2003).

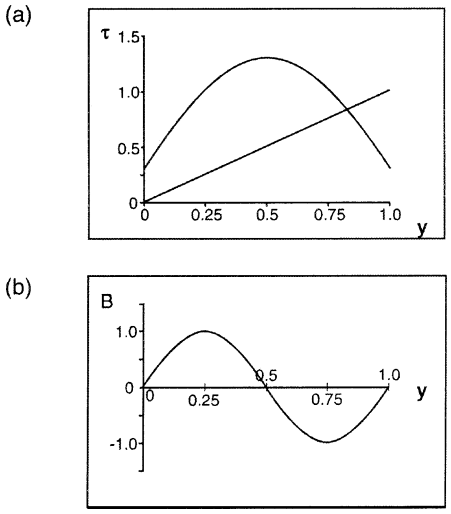

FIG. 4. The assumed forcing functions: (a) wind fields $[\tau_o(y)]/\tau_o = y$ and $\{0.3 + \sin[(\pi y)/L_y]\}$ and (b) buoyancy flux $[\tilde{B}(y)]/\tilde{B}_o = \sin[(2\pi y)/L_y]$, plotted as a function of y/L_y.

It is worthy of note that f appears in Eq. (22) in combination with the wind stress, and so τ_o and f have the same status and could both be allowed to vary: solutions to Eq. (21) can readily be found with variable f. However, the closure assumption, Eq. (16), is based on f-plane ideas and may require modification in the presence of β (see the appendix). For this reason, we confine ourselves here to f-plane solutions.

Reduction of the problem to a system of *ordinary* differential equations, as in Eq. (22), enables analytical expressions for the thermocline depth to be found for simple forcing functions (see section 3c). For more complicated and realistic patterns of forcing, the system of Eq. (22) requires an elementary numerical calculation. Some solutions are presented below in section 3d.

b. Forcing fields

1) WIND

We consider two idealized wind profiles, one that increases linearly from Antarctica:

$$\tau_o(y) = \tau_o(y/L_y), \tag{23}$$

and a second profile with more structure and perhaps more realism:

$$\tau_o(y) = \tau_o\left[0.3 + \sin\left(\frac{\pi y}{L_y}\right)\right]. \tag{24}$$

They are plotted in Fig. 4a. Numerical constants that are assumed are set out in Table 1.

2) SURFACE BUOYANCY AND BUOYANCY FLUX

We suppose that the surface buoyancy field increases linearly away from Antarctica:

TABLE 1. Numerical constants used in solutions for circumpolar flow.

Surface (specific) wind stress	τ_o	2×10^{-4} m^2 s^{-2}
Meridional scale of ACC	L_y	2000 km
Zonal scale of ACC at 55°N	L_x	21 000 km
Vertical scale	H	1 km
Mixed layer depth	h_m	200 m
Coriolis parameter	f	-10^{-4} s^{-1}
Planetary vorticity gradient	β	10^{-11} s^{-1} m^{-1}
Buoyancy change across ACC	Δb_o	7×10^{-3} m s^{-2}
Net buoyancy forcing	$\tilde{B}_o$	2×10^{-9} m^2 s^{-3}
Eddy transfer coefficient	K	500 m^2 s^{-1}
Eddy parameter	$k = \frac{L_y K}{H}$	10^6 m^2 s^{-1}
Thermal expansion coefficient	α	10^{-4} K^{-1}
Specific heat of water	C_p	4000 J kg^{-1} K^{-1}
Density of water	ρ	10^3 kg m^{-3}

$$b_o = \Delta b_o \frac{y}{L_y}, \tag{25}$$

where Δb_o is the buoyancy drop across the ACC at the surface.

The patterns of net buoyancy forcing over the ACC are uncertain. We experiment with the following form:

$$\tilde{B}(y) = \pm \tilde{B}_o \sin\left(\frac{2\pi y}{L_y}\right). \tag{26}$$

If the positive sign is chosen, buoyancy is gained on the polar flank of the ACC and is lost on the equatorial flank, as suggested by the observations—see Speer et al. (2000). Note that the form Eq. (26) ensures that the net buoyancy flux vanishes, when integrated across the jet.

3) NUMERICAL CONSTANTS

Table 1 defines and gives typical values of the parameters used in our calculations. Note that if the thermal expansion coefficient $\alpha = 10^{-4}$ K^{-1} then a $\tilde{B}_o$ of 2×10^{-9} m^2 s^{-3} corresponds to a heat flux of 10 W m^{-2} and a buoyancy jump $\Delta b_o = 7 \times 10^{-3}$ m s^{-2} corresponds to a temperature jump of 10°C.

c. Depth of the thermocline

Integration of the system in Eq. (22) is particularly simple for those characteristics that emanate from the base of the mixed layer at which $\Psi_{\text{res}} = 0$, corresponding to $\tilde{B} = 0$—no net heating of the surface layers. Then Eq. (22) reduces to

$$\frac{dy}{dl} = v_c = 1$$

$$\frac{dz}{dl} = w_c = -\left[-\frac{\tau_o(y)}{fk}\right]^{1/2}. \tag{27}$$

One such characteristic corresponds to the base of the

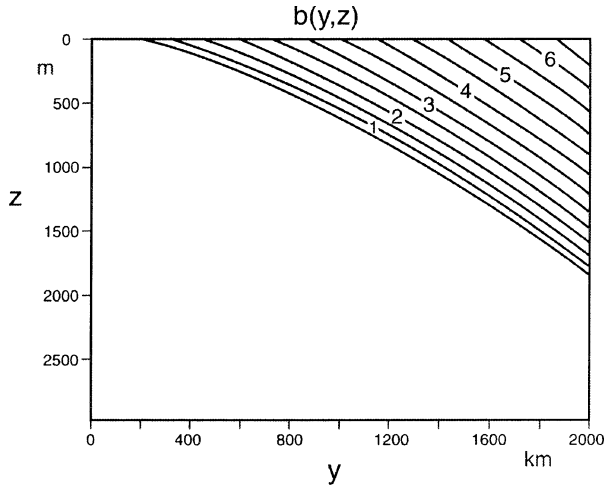

FIG. 5. The stratification $\overline{b}$ obtained for the linear wind profile, Eq. (23), in the case of vanishing Ψ_{res} (contour interval is 10^{-3} m s^{-2}). A linear buoyancy profile is assumed at the sea surface, Eq. (25). The depth of the zero $\overline{b}$ surface is given by the formula Eq. (29). Numerical constants used are set out in Table 1.

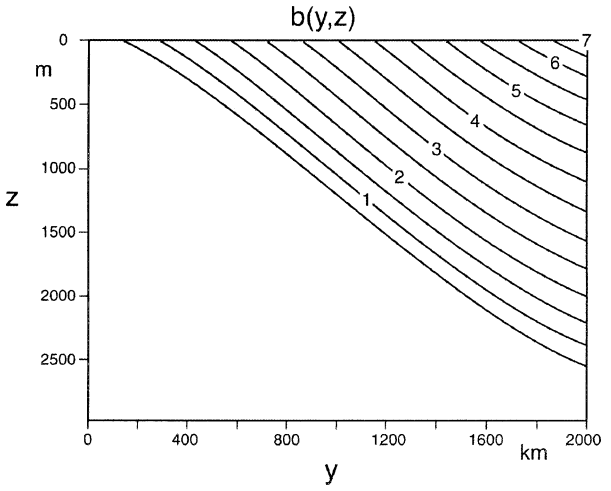

FIG. 6. The stratification $\overline{b}$ (contour interval is 10^{-3} m s^{-2}) obtained for the wind profile, Eq. (24), in the case of vanishing Ψ_{res}. A linear buoyancy profile is assumed at the sea surface, Eq. (25). The assumed numerical constants are set out in the table.

thermocline $z = -h(y)$, which, in our case, is best defined by the isopycnal outcropping at $y = 0$ (where $\overline{b}_o = 0$). Fluid below the thermocline [$z < -h(y)$] is assumed to be homogeneous with vanishing residual circulation: $\Psi_{res} = 0$. The consistency of our assumption that $\Psi_{res} = 0$ at $y = 0$ at the base of the mixed layer is ensured by using the buoyancy forcing function Eq. (26) with $\tilde{B}|_{y=0} = 0$, as required by Eq. (11).

The depth of the thermocline under these assumptions reduces to a first integral of Eq. (27):

$$h(y) = -\int_0^y \left[-\frac{\tau_o(l)}{fk}\right]^{1/2} dl. \tag{28}$$

The fact that the thermocline depth depends on $\sqrt{\tau_o}$ is a consequence of our closure assumption Eq. (17)—also see the appendix where key parametric dependencies are summarized.

For the linear variation of the wind stress $\tau(y) = \tau_o y$, Eq. (28) yields

$$h(y) = -\frac{2}{3}\left(\frac{\tau_o}{fk}\right)^{1/2} L\left(\frac{y}{L}\right)^{3/2} \tag{29}$$

and defines the depth of the deepest $\overline{b}$ surface plotted in Fig. 5. The vertical scale is set by

$$\frac{2}{3}\left(\frac{\tau_o}{fk}\right)^{1/2} L_y = 1886 \text{ m}$$

for the typical parameters set out in Table 1. We see that the depth of the thermocline increases moving away from Antarctica to reach some 1800 m on the northern flank of the jet, not unlike the observations discussed in Karsten and Marshall (2002b); see their Fig. 4.

Solutions for the more realistic wind field in Eq. (24) can be written down but do not take on a simple form.

d. The stratification and overturning circulation

1) $\tilde{B} = 0$: THE LIMIT OF $\Psi_{res} = 0$

Figure 5 shows the $\overline{b}$ field obtained for the wind Eq. (23) when $\tilde{B} = 0$ and so $\Psi_{res} = 0$. The depth of each isopycnal has been computed from Eq. (27); the deepest isopycnal has the form given by Eq. (29). Indeed all isopycnals in Fig. 5 are parallel to one another. This can readily be understood by inspection of Eq. (20): because $\Psi_{res} = 0$, s_ρ only depends on $\tau_o(y)$ and so is independent of depth. Although we keep f constant in our theory, it is helpful to phrase the discussion in terms of potential vorticity (PV). The isentropic PV gradient (IPVG) is $N^2 f(ds_\rho/dz) = 0$ because the $\overline{b}$ surfaces are parallel to one another with f constant.

The stratification is given by

$$N^2 = \overline{b}_z = b_o/h, \tag{30}$$

where b_o is given by Eq. (25) and h by Eq. (29).

As discussed in the appendix, our expressions for thermocline depth and stratification are consistent with the results of Marshall et al. (2002), Karsten et al. (2002), and Cenedese et al. (2004) derived from studies of laboratory and numerical lenses. The relation of these results to those of Bryden and Cunningham (2003) are also discussed.

Figure 6 shows $\overline{b}$ for the wind field Eq. (24): in this case Eq. (27) had to be integrated numerically. The stratification has more structure because of the more complex form of the driving wind field, but again, with PV uniform, all isopycnals are parallel to one another because f is constant.

In these solutions $\Psi_{res} = 0$ and the momentum budget Eq. (18) reduces to

$$\tau_O/f = \Psi^* \tag{31}$$

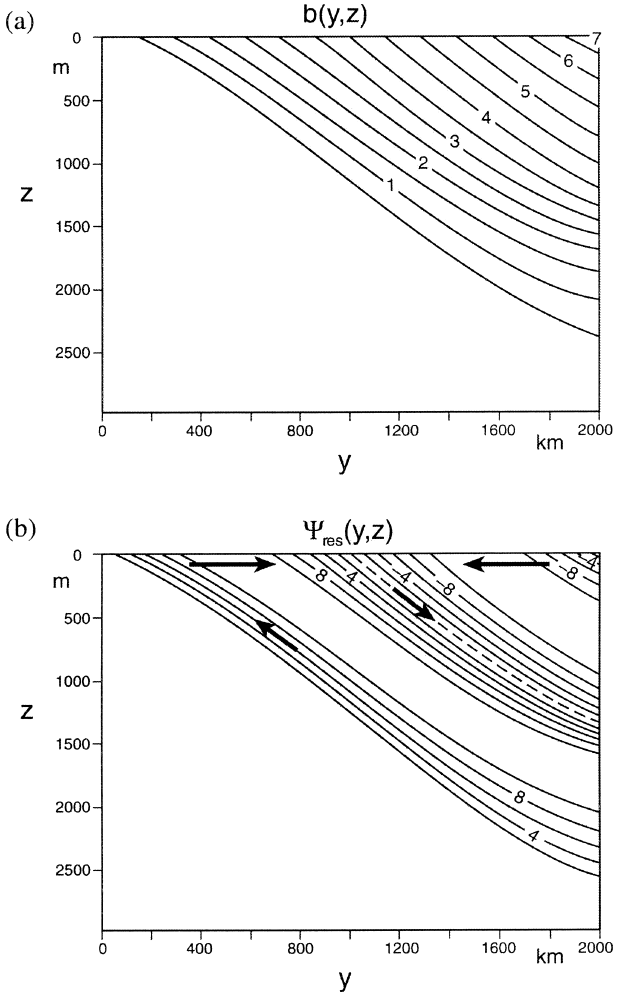

FIG. 7. (a) The buoyancy $\overline{b}$ (contour interval is 10^{-3} m s^{-2}) and (b) residual circulation Ψ_{res} (Sv) for nonzero thermal forcing $\tilde{B} = +\tilde{B}_o \sin[(2\pi y)/L_y]$. The wind stress is given by Eq. (24).

Eddies carry the momentum imparted by the wind vertically through the column by interfacial form drag. The relationship Eq. (31) was first derived heuristically by Johnson and Bryden (1989)—see the discussion in Karsten et al. (2002) and Olbers and Ivchenko (2002). We see it now as a special case of Eq. (13) applicable only in the limit that $\Psi_{res} = 0$.

In the homogeneous layer below the main thermocline $z < -h(y)$ we assume that Ψ^* remains finite (exactly balancing $\overline{\Psi}$) until interaction with topography can balance the surface stress through topographic form drag as described in Munk and Palmen (1951). In this homogeneous layer we set $u = u_{abyss}$ and suppose that

$$\epsilon u_{abyss} = \tau_o. \tag{32}$$

Here ϵ is a parameterization of bottom Ekman layer/topographic form-drag effects.

We now go on to consider effects caused by the *finite* residual circulation by including nonzero buoyancy forcing $\tilde{B}$ of the form in Eq. (26).

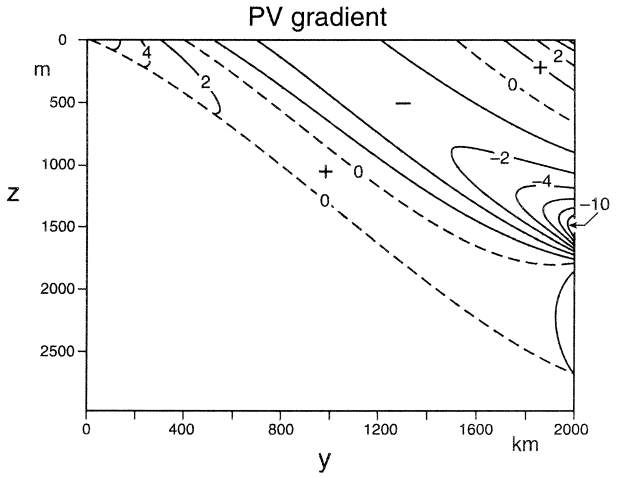

FIG. 8. Isentropic PV gradient normalized by the nominal β-induced contribution (see text) for the solution shown in Fig. 7. Regions of positive IPVG are marked (+); negative regions are marked (−).

2) $\tilde{B} \neq 0$: OVERTURNING CIRCULATION

Figures 7a,b show $\overline{b}$ and Ψ_{res} for the wind field Eq. (24) and the buoyancy forcing given by Eq. (26), choosing the positive sign, and $\tilde{B}_o = 2 \times 10^{-9}$ m^2 s^{-3}, that is, we warm south of the ACC and cool north of it, as suggested by air–sea flux observations. The sense of the residual circulation corresponds to upwelling of fluid in the deepest layers that outcrop at the poleward flank of the ACC ($0 < y < L_y/4$) and the shallow layers that outcrop on its equatorward flank ($3L_y/4 < y < L_y$). At the surface, residual flow converges in to intermediate layers (outcropping at the latitudes $L_y/4 < y < 3L_y/4$), from the south on the poleward flank and from the north on the equatorial flank. Here fluid is subducted downward and equatorward: we associate this flow with Antarctic Intermediate Water.

Note that now isopycnal surfaces are not parallel to one another: the subtle variation in the thickness of isopycnal layers implies the presence of interior PV gradients. The spatial distribution of these PV gradients $(\partial\overline{q}/\partial y)_b = N^2 f(\partial s_\rho/\partial z)$ is shown in Fig. 8, where it is normalized by the nominal value of PV gradient due to β, not used in the theory. We see that the PV gradient reverses sign with v_{res}: fluid upwells as it approaches Antarctica in regions of positive PV gradient and fluid is subducted and flows equatorward in regions of negative PV gradient (we return to this point in the conclusions).

The magnitude of the overturning streamfunction plotted in Fig. 7b is set by the assumed buoyancy gradient and surface buoyancy flux at the sea surface. For the parameters chosen in Table 1 we find

$$\Psi_{res} = \frac{\tilde{B}_o L_y L_x}{\Delta b_o} = 12 \text{ Sv}$$

(where 1 Sv $\equiv 10^6$ m^3 s^{-1}), broadly consistent with the

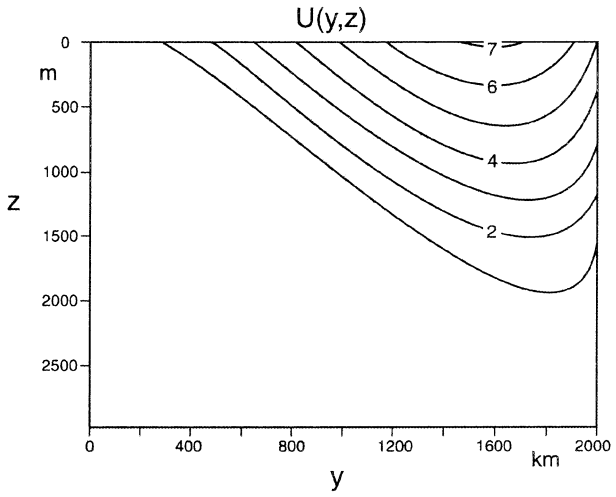

FIG. 9. Vertical cross section of the zonal velocity $\overline{u}(y, z)$ that goes along with the $\overline{b}$ field shown in Fig. 7. The contour interval is 10^{-2} m s^{-1}.

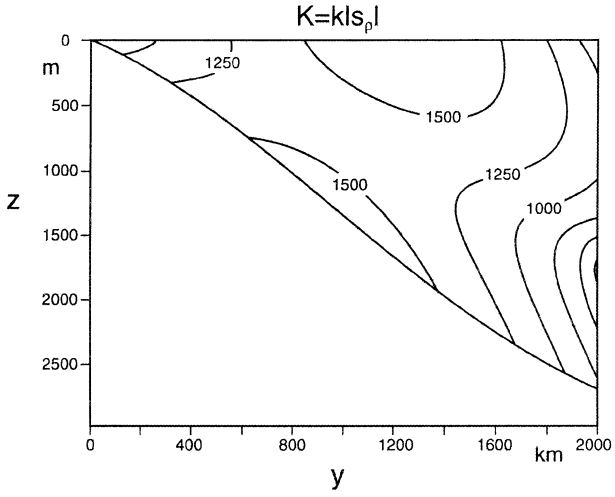

FIG. 10. Contours of the eddy-transfer coefficient K (m^2 s^{-1}). The largest values of K, about 1600 m^2 s^{-1}, occur near the center of the ACC front.

analysis of Marshall (1997) who found residual circulations of 10–15 Sv, but somewhat smaller than the 20 Sv or so of overturning implied by air–sea fluxes—see Karsten and Marshall (2002a). In comparison with the zonal transport (~100 Sv; see below), this flow is weak. We will discuss the processes responsible for $\tilde{B}_o$ below in section 3f.

3) ZONAL TRANSPORT

The large-scale zonal velocity $\overline{u}$ in Fig. 9 was computed from the thermal wind balance assuming no motion below the thermocline [$z < -h(y)$]. The general structure of the thermal wind velocity field has a peak of 7 cm s^{-1}, broadly consistent with the observations (see Fig. 1c). The zonal baroclinic transport directly computed from Fig. 9 is 75 Sv, however, considerable smaller than the observed 130-Sv transport of the ACC. The difference is perhaps due to our uncertainty in the choice of eddy transfer coefficient, the prescribed linear variation in the surface buoyancy, Eq. (25), which does not impose a frontal structure, or simply the idealized nature of the model. Note, however, that to obtain the absolute velocity we should add the depth-independent $u_{\text{abyss}} = [\tau_o(y)]/\epsilon$ to this profile. Gille (2003) estimates a barotropic component to the stream of about 1 cm s^{-1}. If u_{abyss} has a peak value of 1 cm s^{-1}, then the depth-integrated component contributes a transport of 40 Sv to the transport if the current is 3 km deep and $L_y = 2000$ km.

In the limit that $\Psi_{\text{res}} \to 0$, the baroclinic transport of the ACC depends linearly on the wind: this can be shown by integrating up the thermal wind equation, $f\overline{u}_z = \overline{b}_y$, from depth $z = -h$, Eq. (29), to the surface, using Eq. (21) (with $\Psi_{\text{res}} = 0$). The resulting $\overline{u}$ is then integrated vertically and across the stream to obtain the transport. We find that the baroclinic transport depends on external parameters as follows:

$$\text{baroclinic transport} \sim \frac{\tau_o L^2 \Delta b}{f^2 k}. \tag{33}$$

The transfer coefficient $K(y, z) = k|s_\rho|$ plotted in Fig. 10 indicates strong spatial variation in the eddy activity, which, in our model, is mostly limited to the regions of large vertical shear. For the assumed $k = 10^6$ m^2 s^{-1}, the maximum value of K reaches 1600 m^2 s^{-1}, not inconsistent with observational and numerical estimates (see, e.g., Visbeck et al. 1997; Stammer 1998, Karsten and Marshall 2002). Note that the former two papers attempt to estimate a vertically averaged eddy diffusivity over the main thermocline of the ocean, whereas Karsten and Marshall estimate the near-surface diffusivity (which is likely to be elevated above interior values).

e. Meridional eddy heat and buoyancy flux

The meridional eddy buoyancy flux in the limit of vanishing Ψ_{res} is given by Eq. (31):

$$\overline{v'b'} = \overline{b}_z \frac{\tau_o}{f}.$$

If $\overline{b}_z$ is given by Eq. (30) and the windfield by Eq. (23), then the integrated buoyancy flux at midchannel is

$$\int_{-h}^{0} \overline{v'b'}\, dz = \frac{\Delta b_o}{4} \frac{\tau_o}{f}.$$

If the buoyancy flux is dominated by the heat flux (note, however, that freshwater fluxes may make an important contribution in the ACC), then

$$\mathcal{H} = \frac{\rho}{g}\frac{C_p}{\alpha}B,$$

for the parameters given in Table 1.

This value is of the same order as estimated by, for example, de Szoeke and Levine (1981), Marshall et al. (1993), and, most recently, Gille (2003). Note that the above estimate is independent of details of the eddy flux closure because it pertains in the limit that $\Psi_{\text{res}} = 0$ and so Eq. (31) holds. Of course, in the limit that $\Psi_{\text{res}} = 0$, the meridional heat transport by eddies is *exactly* balanced by transport of heat by the mean meridional overturning $\overline{\Psi}$.

The total heat transport across the ACC in our model is a function of the imposed $\tilde{B}_o$, Eq. (12). If there is warming south of the stream and cooling north of the stream—as in the calculations presented here—then $\overline{\Psi}$ carries slightly more heat north than Ψ^* does south.

We now discuss the role of diapycnal eddy heat fluxes in setting the pattern of $\tilde{B}_o$.

f. The role of diapycnal eddy heat fluxes

In the calculations shown thus far, a pattern of buoyancy forcing ($\tilde{B}_o$) was prescribed. It includes contributions from air–sea fluxes (B_o) and from the lateral eddy heat transfer in the mixed layer [see Eq. (12)]. In this section we compute, as part of the solution, the contribution due to mixed layer eddy buoyancy flux given a prescribed surface buoyancy forcing (B_o).

Because the mixed layer is assumed to be vertically homogeneous, the mixed layer eddy fluxes in Eq. (12) can be expressed as a function of the mean quantities immediately below the mixed layer using the interior closure

$$\overline{v'b'} = -K\frac{\partial b_o}{\partial y} = ks_o\frac{\partial b_o}{\partial y}, \tag{35}$$

where $s_o(y) = s_\rho(y, -h_m)$. For the linear surface buoyancy profile Eq. (25), convergence of the eddy flux in Eq. (12) reduces to

$$\frac{\partial \overline{v'b'}}{\partial y} = k\frac{\partial s_o}{\partial y}\frac{\partial b_o}{\partial y}. \tag{36}$$

Using Eq. (17) evaluated at the mixed layer base, Eq. (11) yields $\tilde{B}_o$ as a function of s_o:

$$\tilde{B}_o = \frac{\partial b_o}{\partial y}\left(-ks_o^2 - \frac{\tau}{f}\right). \tag{37}$$

Using Eqs. (37) and (36) to simplify Eq. (12) (setting $\mu = 0$), we obtain the following ordinary differential equation for s_o:

$$h_m\frac{\partial b_o}{\partial y}\frac{\partial s_o}{\partial y} = B_o + \frac{\partial b_o}{\partial y}\left(ks_o^2 + \frac{\tau_o}{f}\right), \tag{38}$$

which can be solved given a distribution of B_o, τ_o, b_o, and f. Integration of the first-order differential Eq. (38) requires a single boundary condition; if $\Psi_{\text{res}} = 0$ at the base of the mixed layer at $y = 0$, then Eq. (20) tells us that

$$s_o(0) = -\left[\frac{\tau_o(0)}{fk}\right]^{1/2}. \tag{39}$$

Figure 11a presents the numerical solution of Eqs. (38) and (39) in the case that the surface buoyancy forcing vanishes ($B_o = 0$) and for the wind profile given by Eq. (24); other parameters are the same as were used to obtain Fig. 7. The solution is expressed in Fig. 11a in terms of the total buoyancy flux $\tilde{B}_o$, which has been computed from s_o using Eq. (37). Thus Fig. 11a shows that, as is to be expected from downgradient diffusion in Eq. (35), eddy heat transfer in the mixed layer warms the poleward flank of the ACC and cools the equatorial flank. This pattern is consistent with the one assumed for $\tilde{B}_o$ a priori in section 3d. Addition of a finite surface flux in Fig. 11b modifies $\tilde{B}$ but, for a realistic parameter range, does not change the general structure of the total buoyancy flux.[4]

Figures 12a,b show the buoyancy field and residual circulation computed using the method of characteristics (see section 3a) for the buoyancy forcing in Fig. 11a. The overturning circulation plotted in Fig. 12b, reaching a magnitude of some 6 Sv, is entirely driven by diabatic eddy processes—the air–sea flux is assumed to be zero. We see, then, that diabatic eddy effects may make a nontrivial contribution to the residual-mean overturning in the ACC.

4. Discussion and conclusions

We have applied zonal average residual mean theory to develop a model of the ACC that combines the effects

$$\text{meridional heat flux} = \frac{1}{4}\frac{\rho}{g}\frac{C_p}{\alpha}\Delta b_o\frac{\tau_o}{f}L_x = 0.3 \times 10^{15}\ \text{W} \tag{34}$$

[4] There is no reason to assume a priori that the combined effect of surface buoyancy forcing and eddies in Fig. 11b is a linear superposition of these two contributions. The governing equation [Eq. (38)] is significantly nonlinear. Nevertheless, in the parameter range under consideration, the two contributions add linearly.

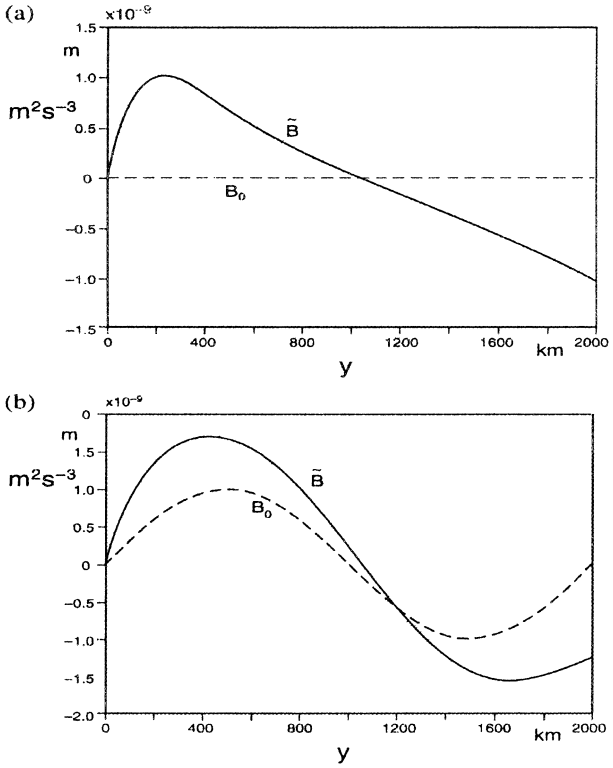

FIG. 11. Total buoyancy flux $\tilde{B}_o$ (solid line) computed for a given air–sea flux B_o (dashed line). (a) The $\tilde{B}_o$ when $B_o = 0$: in this case diabatic eddy fluxes redistribute buoyancy within the mixed layer. (b) The $\tilde{B}_o$ when $B_o = B_o \sin[(2\pi y)/L_y]$, with $B_o = 1 \times 10^{-9}$ m^2 s^{-3}.

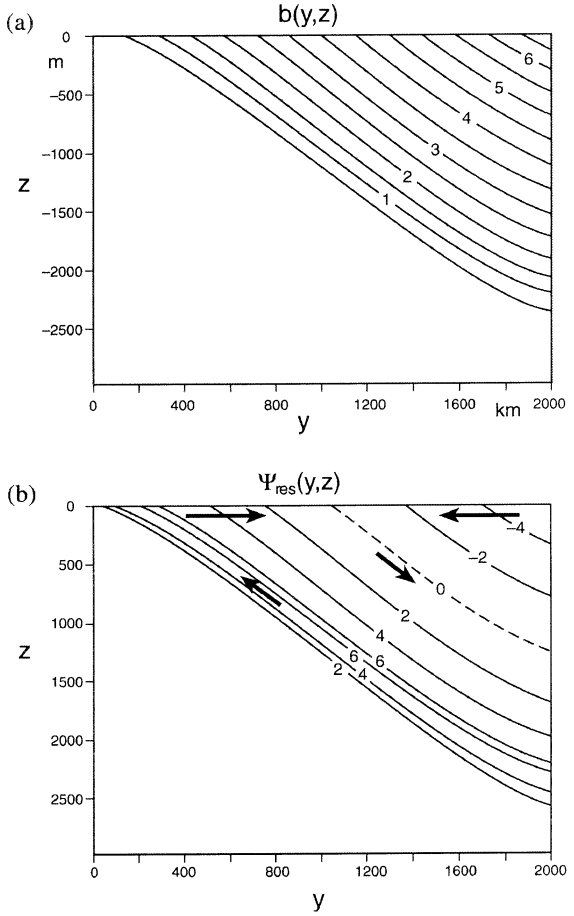

FIG. 12. (a) The buoyancy field and (b) the residual circulation for the buoyancy forcing shown in Fig. 11a. The wind stress is given by Eq. (24). Contour intervals are $\overline{b} = 10^{-3}$ m s^{-2} and $\Psi_{res} = 2$ Sv, respectively. Here the residual overturning streamfunction, Fig. 11b, is driven entirely by diabatic eddy fluxes in the mixed layer.

of buoyancy and mechanical forcing in a transparent way. Simple solutions have been derived on the f plane that capture its mean buoyancy distribution, zonal current, and pattern of meridional overturning circulation. In our theory, transfer by baroclinic eddies balances imposed patterns of wind and buoyancy forcing and

1) controls the depth to which the thermocline of the ACC penetrates; and
2) plays, through diabatic fluxes directed horizontally through the mixed layer, an important role in redistributing buoyancy in the mixed layer, supporting a meridional overturning circulation, surface convergence at the axis of the ACC, and subduction.

We find that the depth of the thermocline and baroclinic transport is intimately connected to the assumed balance between the applied wind stress and vertical momentum transfer by baroclinic eddies [see Eq. (28)]. The overturning circulation Ψ_{res}, by contrast, is associated with buoyancy supply to and from the mixed layer $\tilde{B}$ [see Eq. (11)] in which both air–sea flux and diabatic eddy fluxes play a role.

a. Thermocline depth, stratification, and zonal transport

If Ψ^* depends on the square of the isopycnal slope, as assumed in Eq. (17), and Ψ_{res} is smaller than its component parts, then the depth of the thermocline depends on the square root of the wind stress [see Eq. (28)] and the stratification is given by Eq. (30). This result finds support in laboratory (Marshall et al. 2002; Cenedese et al. 2004) and numerical studies (Karsten et al. 2002) of the ACC. A corollary of this result is that the zonal transport depends linearly on the applied wind [see Eq. (33)]. This dependence should be compared with the predictions of other authors who argue that the baroclinic transport varies like $\sqrt{\tau}$ (Johnson and Bryden 1989), is independent of the wind (Straub 1993), or varies like τ (Gnanadesikan and Hallberg 2000; Karsten et al. 2002, and this study). Only in the latter two studies is the stratification not set a priori.

We note the dependence of our solutions on the form assumed for our eddy closure and that of the eddy transfer coefficient, Eqs. (15) and (16). The eddy closure assumption $\overline{v'b'} = -K\partial\overline{b}/\partial y$ is conventional and finds support in eddy-resolving numerical models of the ACC—see, for example, the recent study of Karsten et

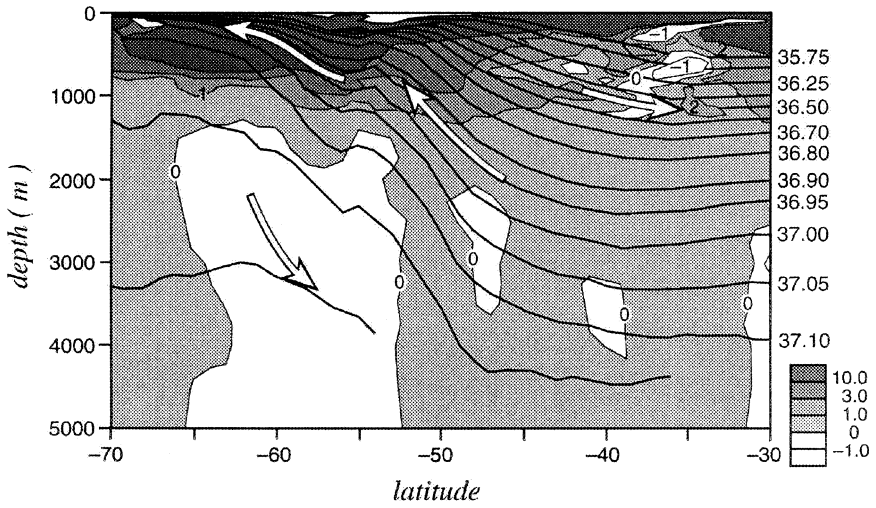

FIG. 13. The meridional IPVG deduced from a hydrographic data base by Marshall et al. (1993). Regions of positive IPVG are shaded gray; regions of negative IPVG are white. The arrows mark the sense of the sense of the implied residual flow; poleward where IPVG > 0, equatorward where IPVG < 0. Note that the downward arrow around Antarctica is hinted at by the sign of the (very weak) IPV gradient but is not represented in the simple solutions discussed here.

al. (2002). The assumed dependence of K on the local baroclinity yields a simple but important connection between K and mean flow quantities, as described in the appendix. It is, however, an f-plane closure that may be modified by the presence of β, see below.

b. Meridional overturning circulation

The sense of the residual circulation shown in Fig. 7b corresponds to upwelling of fluid in the deepest layers that outcrop at the poleward flank of the ACC and the shallow layers that outcrop on its equatorward flank. At the surface, fluid converges in to intermediate layers, from the south on the poleward flank and from the north on the equatorward flank. It is tempting to associate the fluid upwelling around Antarctica with upper North Atlantic Deep Water and the fluid subducted downward from the convergence zone farther north with Antarctic Intermediate Water. On the equatorward flank of the ACC, the residual flow is to the south (for our chosen pattern of $\tilde{B}$ in Fig. 4b), and so the eddy-induced mixed layer transport here is larger than, and in the opposite direction to, the Ekman transport. This situation is not implausible—see, for example, the inference from observations of these components by Karsten and Marshall (2002). The strength (and sense) of the overturning circulation is of approximately 10 Sv and depends on our choice for the magnitude of $\tilde{B}$. Note that our solution does not contain a representation of Antarctic Bottom Water because of the absence of cooling around Antarctica in the assumed $\tilde{B}$.

The large-scale potential vorticity field is a primary contact point between our theory and the observations. Interior residual flow v_{res} is only possible if there is a meridional eddy PV flux, $\overline{v'q'}$: $-fv_{\text{res}} = \overline{v'q'}$. If $\overline{v'q'}$ is fluxed down the isentropic PV (IPV) gradient, then $v_{\text{res}} = -(K/f)(\partial\text{IPV}/\partial y)$. Thus the sense of v_{res} can be gleaned from inspection of observations of the meridional IPV gradient. The arrows in Fig. 13 [modified from Marshall et al. (1993)] indicate the sense of the implied residual flow, poleward where IPV increases poleward and equatorward where IPV increases equatorward. The shallow regions of reversed IPVG seen in the observations are very likely to be associated with low-PV fluid created by convection in mode-water formation just equatorward of the ACC. These convected waters are subducted in to the interior, carrying with them their low-PV signal and reversing the sign of IPV.

c. The role of β

As discussed in the appendix, our eddy closure, Eqs. (15) and (16), is explicitly an f-plane parameterization, with no sense of a critical shear for instability or eddy saturation. This closure may break down in the ACC where β constraints are likely to be important—see, for example, Tansley and Marshall (2001) or Hallberg and Gnanadesikan (2001). Further study is required to draw such effects in to our theory.

Last, we emphasize that the ideas and formulation set out here have no direct counterpart in thermocline theory. Our solutions are not in Sverdrup balance because there is no β effect. Because of the absence of meridional boundaries, pathways for mean heat transport across the ACC are limited, and so eddies must be largely responsible for poleward heat transport across the stream (see, e.g., de Szoeke and Levine 1981). The eddies also balance the input of momentum by the winds. The southward heat flux is directly related to a downward momentum flux through interfacial drag (see, e.g.,

Johnson and Bryden 1989). This drag allows the surface momentum to be transferred to depth where it can be dissipated by mountain drag as the ACC flows over the high ridges (Munk and Palmen 1951). Such a balance has been established as the dominant balance of the ACC both in observations (Phillips and Rintoul 2000) and in numerical models (Ivchenko et al. 1996; Gille 1997) and is at the heart of the simple model presented here.

Tasks for the future are (i) to incorporate the effects of the β effect, (ii) to unravel the zonal-average 2D solutions discussed here to study the effect of regional topographic and forcing detail, and (iii) to study the role of interior mixing.

Acknowledgments. This work was greatly helped by numerous conversations about residual-mean theory and the ACC with our colleague Alan Plumb. Two anonymous referees and Richard Karsten made very helpful comments on the manuscript. We acknowledge the support of the physical oceanography program of NSF.

APPENDIX

Eddy Closure and Scaling Results

To place the eddy closure adopted in this study in context [Eq. (16)] and to relate our results to previous work, following Visbeck et al. (1997) [using ideas that go back to Green (1970)] we write the eddy transfer coefficient as follows:

$$K = \overline{v'l'} = c_e \frac{f}{\sqrt{\mathrm{Ri}}} L_\rho L_y, \tag{A1}$$

where c_e is a constant, $\mathrm{Ri} = (N^2h^2)/u^2$ is the Richardson number, u is the mean zonal current at the surface, $f/\sqrt{\mathrm{Ri}}$ is the Eady growth rate, $L_\rho = (Nh)/f$ is the deformation radius, and L_y is the meridional scale of the baroclinic zone. As discussed in, for example, Marshall et al. (2002), the eddy velocity implied by Eq. (A1) is $v' \sim (f/\sqrt{\mathrm{Ri}})L_\rho = u$, appropriate if the eddies garner energy over a deformation scale L_ρ (see, e.g., the discussion in Held 1999). The eddy transfer scale is assumed to be L_y, the scale of the baroclinic zone. Note that this may be a problematical assumption in the ACC—the eddy transfer scale could be set, for example, by the Rhines scale $(u/\beta)^{1/2}$, an obvious avenue for future enquiry.

The thermal wind equation tells us that

$$u = \frac{h}{f}\frac{\Delta b_o}{L_y}, \tag{A2}$$

where Δb_o is the buoyancy change at the surface over the scale L_y. Hence K, Eq. (A1), can be written as

$$K = c_e u L_y = c_e \frac{h \Delta b_o}{f}. \tag{A3}$$

Further, from Eq. (16) and supposing that $|s_\rho| = h/L_y$, we can identify k as

$$k = c_e \frac{\Delta b_o L_y}{f}. \tag{A4}$$

Using Eq. (A4) our predicted depth of the thermocline, Eq. (29) can then be written entirely in terms of external parameters as

$$h \sim \left(\frac{\tau_o L_y}{\Delta b_o}\right)^{1/2}. \tag{A5}$$

Furthermore, if we assert that $B_o \sim w_{\mathrm{Ek}} \Delta b_o$ with $w_{\mathrm{Ek}} = \tau_o/(fL_y)$ being the scale of the Ekman pumping, Eq. (A5) can be expressed in terms of buoyancy forcing B_o, rather than the surface buoyancy field Δb_o; thus

$$h \sim \left(\frac{f}{B_o}\right)^{1/2} w_{\mathrm{Ek}} L_y. \tag{A6}$$

This equation is the scaling for thermocline depth discussed in Marshall et al. (2002) and Karsten et al. (2002) and derived from their studies of labaratory and numerical lenses forced by buoyancy flux rather than a prescribed buoyancy field. It is interesting to note that the baroclinic transport, Eq. (33), scales like $\sim(\tau_o L)/f$, independent of Δb_o, if Eq. (A4) is subsituted for k.

Last we relate the above expressions to those discussed in Bryden and Cunningham (2003). The stratification implied by the Marshall et al. (2002) scaling, Eq. (A6), is

$$N^2 = \frac{\Delta b_o}{h} \sim \frac{B_o^{2/3}}{w_{\mathrm{Ek}}^2 f^{1/2} L_y} \sim \frac{f^2 B_o}{\tau_o^2} K,$$

where we have set $\Delta b_o = B_o/w_{\mathrm{Ek}}$ and used Eqs. (A3) and (A6) to express K as $K = c_e(B_o/f)^{1/2}L_y$. The relation $N^2 = [(f^2B_o)/\tau_o^2]K$ is the key result of Bryden and Cunningham (2003), their Eq. (9).

REFERENCES

Andrews, D. G., J. Holton, and C. Leovy, 1987: *Middle Atmosphere Dynamics.* Academic Press, 489 pp.

Bryden, H. L., 1979: Poleward heat flux and conversion of available potential energy in Drake Passage. *J. Mar. Res.*, **37,** 1–22.

——, and S. A. Cunningham, 2003: How wind-forcing and air–sea heat exchange determine the meridional temperature gradient and stratification for the Antarctic Circumpolar Current. *J. Geophys. Res.*, **108,** 3275, doi:10.1029/2001JC001296.

Cenedese, J., J. Marshall, and J. A. Whitehead, 2004: A laboratory model of thermocline depth and exchange fluxes across circumpolar fronts. *J. Phys. Oceanogr.*, in press.

de Szoeke, R. A., and M. D. Levine, 1981: The advective flux of heat by mean geostrophic motions in the Southern Ocean. *Deep-Sea Res.*, **28,** 1057–1084.

Doos, K., and D. Webb, 1994: The Deacon cell and other meridional cells of the Southern Ocean. *J. Phys. Oceanogr.*, **24,** 429–442.

Gent, P. R., and J. C. McWilliams, 1990: Isopycnal mixing in ocean circulation models. *J. Phys. Oceanogr.*, **20,** 150–155.

Gille, S., 1997: The Southern Ocean momentum balance: Evidence for topographic effects from numerical model output and altimeter data. *J. Phys. Oceanogr.*, **27,** 2219–2231.

——, 2003: Float observations of the Southern Ocean. Part II: Eddy fluxes. *J. Phys. Oceanogr.,* **33,** 1167–1181.
Gnanadesikan, A., and R. Hallberg, 2000: On the relationship of the Circumpolar Current to Southern Hemisphere winds in coarse-resolution ocean models. *J. Phys. Oceanogr.,* **30,** 2013–2034.
Green, J. S. A., 1970: Transfer properties of the large-scale eddies and the general circulation of the atmosphere. *Quart. J. Roy. Meteor. Soc.,* **96,** 157–185.
Hallberg, R., and A. Gnanadesikan, 2001: An exploration of the role of transient eddies in determining the transport of a zonally reentrant current. *J. Phys. Oceanogr.,* **31,** 3312–3330.
Held, I., 1999: The macroturbulence of the troposphere. *Tellus,* **51A-B,** 59–70.
——, and T. Schneider, 1999: The surface branch of the zonally averaged mass transport circulation of the troposphere. *J. Atmos. Sci.,* **56,** 1688–1697.
Ivchenko, V. O., K. J. Richards, and D. P. Stevens, 1996: The dynamics of the Antarctic Circumpolar Current. *J. Phys. Oceanogr.,* **26,** 753–774.
Johnson, G. C., and H. L. Bryden, 1989: On the size of the Antarctic Circumpolar Current. *Deep-Sea Res.,* **36,** 39–53.
Karsten, R., and J. Marshall, 2002a: Constructing the residual circulation of the Antarctic Circulation Current from observations. *J. Phys. Oceanogr.,* **32,** 3315–3327.
——, and ——, 2002b: Testing theories of the vertical stratification of the ACC against observations. *Dyn. Atmos. Oceans,* **36,** 233–246.
——, H. Jones, and J. Marshall, 2002: The role of eddy transfer in setting the stratification and transport of a circumpolar current. *J. Phys. Oceanogr.,* **32,** 39–54.
Marshall, D., 1997: Subduction of water masses in an eddying ocean. *J. Mar. Res.,* **55,** 201–222.
Marshall, J. C., 1981: On the parameterization of geostrophic eddies in the ocean. *J. Phys. Oceanogr.,* **11,** 1257–1271.
——, D. Olbers, H. Ross, and D. Wolf-Gladrow, 1993: Potential vorticity constraints on the dynamics and hydrography of the Southern Ocean. *J. Phys. Oceanogr.,* **23,** 465–487.
——, H. Jones, R. Karsten, and R. Wardle, 2002: Can eddies set ocean stratification? *J. Phys. Oceanogr.,* **32,** 26–38.
McWilliams, J. C., W. R. Holland, and J. H. S. Chow, 1978: A description of numerical Antarctic Circumpolar Currents. *Dyn. Atmos. Oceans,* **2,** 213–291.
Munk, W. H., and E. Palmen, 1951: Note on the dynamics of the Antarctic Circumpolar Current. *Tellus,* **3,** 53–55.
Olbers, D., and V. O. Ivchenko, 2001: Diagnosis of the residual circulation in the Southern Ocean as simulated in POP. *Ocean Dyn.,* **52,** 79–93.
Pedlosky, J., 1996: *Ocean Circulation Theory.* Springer-Verlag, 453 pp.
Phillips, H. E., and S. R. Rintoul, 2000: Eddy variability and energetics from direct current measurements of the Antarctic Circumpolar Current south of Australia. *J. Phys. Oceanogr.,* **30,** 3050–3076.
Rhines, P. B., 1993: Ocean general circulation: Wave and advection dynamics. *Modelling Oceanic Climate Interactions,* J. Willebrand and D. L. T. Anderson, Eds., Springer-Verlag, 67–149.
Rintoul, S., C. Hughes, and D. Olbers, 2001: The Antarctic Circumpolar Current system—Chapter 4.6. *Ocean Circulation and Climate,* G. Siedler, J. Church, and J. Gould, Eds., International Geophysics Series, Vol. 77, Academic Press, 271–302.
Speer, K., S. R. Rintoul, and B. Sloyan, 2000: The diabatic Deacon cell. *J. Phys. Oceanogr.,* **30,** 3212–3222.
Stammer, D., 1998: On eddy characteristics, eddy mixing and mean flow properties. *J. Phys. Oceanogr.,* **28,** 727–739.
Straub, D. N., 1993: On the transport and angular momentum balance of channel models of the Antarctic Circumpolar Current. *J. Phys. Oceanogr.,* **23,** 776–782.
Sverdrup, H. U., M. W. Johnson, and R. H. Fleming, 1942: *The Oceans, Their Physics, Chemistry, and General Biology.* Prentice Hall, 1087 pp.
Tansley, C. E., and D. P. Marshall, 2001: On the dynamics of wind-driven circumpolar currents. *J. Phys. Oceanogr.,* **31,** 3258–3273.
Treguier, A. M., I. M. Held, and V. D. Larichev, 1997: On the parameterization of quasi-geostrophic eddies in primitive equation models. *J. Phys. Oceanogr.,* **27,** 567–580.
Visbeck, M., J. Marshall, T. Haine, and M. Spall, 1997: Specification of eddy transfer coefficients in coarse-resolution ocean circulation models. *J. Phys. Oceanogr.,* **27,** 381–402.